Estimation of Total Outgoing Longwave Radiation (OLR) Flux from Geostationary Meteorological Satellite Infrared Window Radiance

Toshiyuki Kurino* and Akihiro Uchiyama**

Abstract

Total outgoing longwave radiation (OLR) flux thermally emitted from the earth-atmosphere system was estimated by applying linear regression equations relating with Geostationary Meteorological Satellite (GMS) Infrared window radiance. These coefficients of regression equations were determined from the results of radiative transfer model simulation on various atmospheric conditions. In this study, OLR radiances were calculated for 140-divided longwave spectral intervals on 140 atmospheric conditions at eight zenith angles.

It was found that there was rather high correlation (R = 0.971) between the total OLR flux from radiative transfer calculations and estimated ones from GMS Infrared window radiance, though there contain low correlation spectral regions corresponding to absorption bands (e.g. watervapor, carbon dioxide, ozone).

1. Introduction

The total OLR flux thermally emitted from the earth-atmosphere system is an important variable, not only as a component of radiation budget but also as an index representing variations of meteorological parameters such as cloud cover and surface temperature.

At the Meteorological Satellite Center (MSC), five-day mean equivalent blackbody temperature (T_{BB}) has been derived from GMS IR window radiance and averaged over 2.5 degrees latitude by 2.5 degrees longitude boxes. This data are subsequently processed into contour map and disseminated to the Headquarters of JMA. Though it has been utilized for the long-range forecast and the climate research

works, there are some problems in the derivation of T_{BB}. Major problems are as follows;

(a) T_{BB} is not derived from whole IR region radiance, but from IR window radiance of GMS as follows;

$$R_{GMS} = \frac{\int_{\nu_1}^{\nu_2} \phi(\nu)*B(\nu, T_{BB})d\nu}{\int_{\nu_1}^{\nu_2} \phi(\nu)d\nu} \qquad (1.1)$$

where R_{GMS} is the IR window radiance of the GMS,

ν_1 and ν_2 are both sides of the IR window (ν_1 = 10.5 μm, ν_2 = 12.5 μm), B (ν, T_{BB}) is the Planck's function at ν and T_{BB}, and $\phi(\nu)$ is spectral response function of GMS IR sensor.

(b) There is no correction procedure for "limb darkening" effect in the derivation of T_{BB}.

To solve these problems, the algorithm of estimating total OLR flux from GMS IR

*Meteorological Satellite Center
　気象衛星センター　システム管理課
**Meteorological Research Institute
　気象研究所　気候研究部

window radiance was developed by applying regression equations. These coefficients of regression equations were determined by simulation using a radiative transfer model on various observed atmospheric conditions.

2. Radiative Transfer Model Simulation

2.1 Atmospheric Condition Data Set

In making the atmospheric condition data set, 140 radiosonde sounding data from widely (latitudinally and geographically) distributed observation stations (see Fig. 1) in all seasons are selected.

The vertical profile of temperature was obtained from those radiosonde observation data. Humidity was extrapolated above the tropopause level with constant relative humidity 2%.

The ozone distribution was estimated from ozonsonde observation data at SAPPORO, TATENO and KAGOSHIMA.

The existence of clouds was judged from the vertical atmospheric profile and concurrent GMS infrared/visible pictures, and then suitable cloud top heights were assigned.

2.2. Simulation Model Calculation

For this model calculation, we followed the same method and algorithm of YAMANOUCHI et al. (1981).

Calculations were performed by using the method of Rodgers and Walshaw (1966). The Goody random model was used in estimating the transmission function and as for the angle integration of the flux transmission function, a diffusivity factor of 1.66 was used.
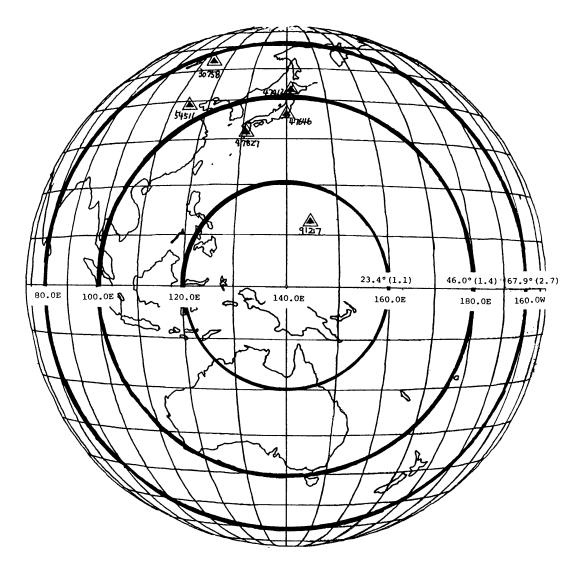
These calculations were performed on the data sets described in section 2.1; 140 atmospheres at eight satellite zenith angles (sec θ = 1.00, 1.25, 1.50, 1.66, 1.75, 2.00, 2.25 and 2.50). 15 mb level was taken as the top of the model atmosphere and the atmosphere was then divided into 40 layers. In this model,

assigned clouds are assumed to be black.

Actual calculations were done respectively in 140 spectral intervals of 10 to 25 cm^{-1} width (see Table 1). The spectral data used in this calculation were; H_2O rotational band (0 − 800 cm^{-1}), 6.3 μm band (1200 − 2200 cm^{-1}), CO_2 15 μm band (520 − 840 cm^{-1}), 4.3, 4.8 and 5.2 μm bands (1800 − 2450 cm^{-1}), O_3 rotational band (0 − 160 cm^{-1}), 14 μm band (610 − 800 cm^{-1}), 9.6 μm band (950 − 1180 cm^{-1}) and H_2O continuum absorption (750 − 1200 cm^{-1}). Line parameters for these absorption bands were derived from the compilation of AFCRL line parameters by McClatchey et al. (1973).

2.3. Example of Simulation

The results of calculated radiances of each longwave spectral interval at satellite zenith angle of secθ = 1.00 were averaged for 140 atmospheres (see Fig. 2). In this figure, Planck's radiances at the indicated temperatures (250, 260 and 270K) are also shown. It is found that mean calculated radiances in IR window region corresponded to Planck's radiances at about 270K.

Calculated limb-darkening effect are shown in Fig. 3. The ratio of the radiance in the direction of the satellite zenith angle θ to that in the local vertical direction (sec θ = 1.00) is plotted for angle values up to sec θ = 2.5. The mean value is also drawn in solid line. Fig. 3 (a) shows the case for IR window radiance and (b) is for total IR radiance. It is found that, against our suspicion, there is little limb-darkening effect in the IR window region. For the whole IR region, however, the limb-darkening effect becomes dominates with the increase of the satellite zenith angle.

Index Number	Station Name	Latitude (degree N)	Longitude (degree E)	Elevation (m)
30758	CITA	52.01	113.20	685
47412	SAPPORO	43.03	141.20	19
54511	BEIJING	39.48	116.28	32
47646	TATENO	36.03	140.08	31
47827	KAGOSHIMA	31.34	130.33	5
91217	GUAM	13.33	144.50	111

Fig. 1. Location of aerological observation stations used for the determination of the atmospheric condition data set. Circles show the equal satellite zenith angle: degrees $(\sec\theta)$.
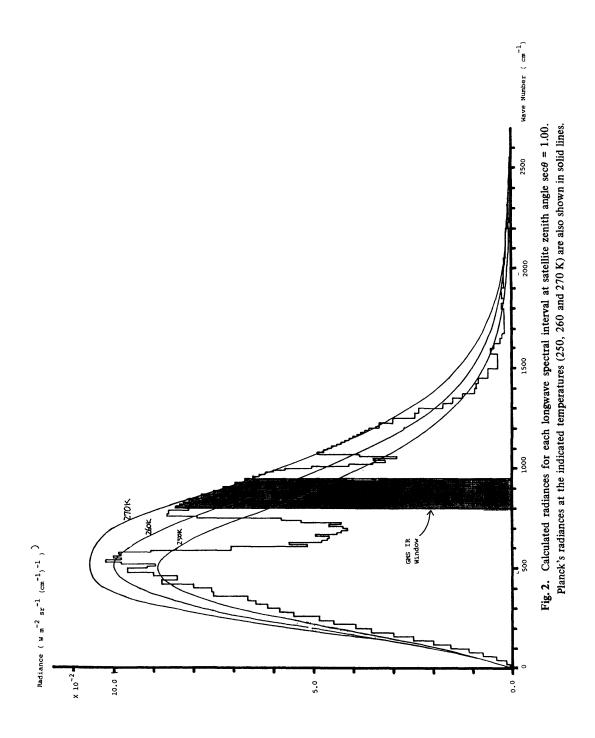
Table 1 Intervals of divided longwave spectral band used in the calculation model. GMS IR window channel is also shown.

	Band Limits (cm^{-1})			Band Limits (cm^{-1})		
1	0.0 -	20.0	36	600.0 -	610.0	
2	20.0 -	40.0	37	610.0 -	620.0	
3	40.0 -	60.0	38	620.0 -	630.0	
4	60.0 -	80.0	39	630.0 -	640.0	
5	80.0 -	100.0	40	640.0 -	650.0	
6	100.0 -	120.0	41	650.0 -	660.0	
7	120.0 -	140.0	42	660.0 -	670.0	
8	140.0 -	160.0	43	670.0 -	680.0	
9	160.0 -	180.0	44	680.0 -	690.0	
10	180.0 -	200.0	45	690.0 -	700.0	
11	200.0 -	220.0	46	700.0 -	710.0	
12	220.0 -	240.0	47	710.0 -	720.0	
13	240.0 -	260.0	48	720.0 -	730.0	
14	260.0 -	280.0	49	730.0 -	740.0	
15	280.0 -	300.0	50	740.0 -	750.0	
16	300.0 -	320.0	51	750.0 -	760.0	
17	320.0 -	340.0	52	760.0 -	770.0	
18	340.0 -	360.0	53	770.0 -	780.0	
19	360.0 -	380.0	54	780.0 -	790.0	
20	380.0 -	400.0	55	790.0 -	800.0	
21	400.0 -	420.0	56	800.0 -	810.0---+	
22	420.0 -	440.0	57	810.0 -	820.0	:
23	440.0 -	460.0	58	820.0 -	830.0	:
24	460.0 -	480.0	59	830.0 -	840.0	:
25	480.0 -	500.0	60	840.0 -	850.0	: GMS IR Window
26	500.0 -	510.0	61	850.0 -	870.0	: Channel
27	510.0 -	520.0	62	870.0 -	890.0	:
28	520.0 -	530.0	63	890.0 -	910.0	:
29	530.0 -	540.0	64	910.0 -	930.0	:
30	540.0 -	550.0	65	930.0 -	950.0---+	
31	550.0 -	560.0	66	950.0 -	960.0	
32	560.0 -	570.0	67	960.0 -	970.0	
33	570.0 -	580.0	68	970.0 -	980.0	
34	580.0 -	590.0	69	980.0 -	990.0	
35	590.0 -	600.0	70	990.0 -	1000.0	

	Band Limits (cm^{-1})			Band Limits (cm^{-1})
71	1000.0 - 1010.0		106	1575.0 - 1600.0
72	1010.0 - 1020.0		107	1600.0 - 1625.0
73	1020.0 - 1030.0		108	1625.0 - 1650.0
74	1030.0 - 1040.0		109	1650.0 - 1675.0
75	1040.0 - 1050.0		110	1675.0 - 1700.0
76	1050.0 - 1060.0		111	1700.0 - 1725.0
77	1060.0 - 1070.0		112	1725.0 - 1750.0
78	1070.0 - 1080.0		113	1750.0 - 1775.0
79	1080.0 - 1090.0		114	1775.0 - 1800.0
80	1090.0 - 1100.0		115	1800.0 - 1825.0
81	1100.0 - 1110.0		116	1825.0 - 1850.0
82	1110.0 - 1120.0		117	1850.0 - 1875.0
83	1120.0 - 1130.0		118	1875.0 - 1900.0
84	1130.0 - 1140.0		119	1900.0 - 1925.0
85	1140.0 - 1150.0		120	1925.0 - 1950.0
86	1150.0 - 1160.0		121	1950.0 - 1975.0
87	1160.0 - 1170.0		122	1975.0 - 2000.0
88	1170.0 - 1180.0		123	2000.0 - 2025.0
89	1180.0 - 1190.0		124	2025.0 - 2050.0
90	1190.0 - 1200.0		125	2050.0 - 2075.0
91	1200.0 - 1225.0		126	2075.0 - 2100.0
92	1225.0 - 1250.0		127	2100.0 - 2125.0
93	1250.0 - 1275.0		128	2125.0 - 2150.0
94	1270.0 - 1300.0		129	2150.0 - 2175.0
95	1300.0 - 1325.0		130	2175.0 - 2200.0
96	1325.0 - 1350.0		131	2200.0 - 2225.0
97	1350.0 - 1375.0		132	2225.0 - 2250.0
98	1375.0 - 1400.0		133	2250.0 - 2275.0
99	1400.0 - 1425.0		134	2275.0 - 2300.0
100	1425.0 - 1450.0		135	2300.0 - 2325.0
101	1450.0 - 1475.0		136	2325.0 - 2350.0
102	1475.0 - 1500.0		137	2350.0 - 2375.0
103	1500.0 - 1525.0		138	2375.0 - 2400.0
104	1525.0 - 1550.0		139	2400.0 - 2425.0
105	1550.0 - 1575.0		140	2425.0 - 2450.0

Fig. 2. Calculated radiances for each longwave spectral interval at satellite zenith angle $\sec\theta = 1.00$. Planck's radiances at the indicated temperatures (250, 260 and 270 K) are also shown in solid lines.

(b)

(a)

Fig. 3. Calculated limb-darkening effect. The ratio of the radiance in the direction of the satellite
zenith angle　to that in the local vertical direction (secθ = 1.00) is shown.
(a) : for IR window radiance
(b) : for total IR radiance

3. Regression Equations in the case of GMS IR Window Radiance

Using these simulated data, equations which relate the total OLR flux to the GMS IR window radiance were derived according to the following steps.

3.1. Regression from Satellite Observed IR Window Radiance to Previously-Set Common IR Window Radiance

The IR radiance observed by the satellite is filtered before arriving to the sensor of the radiometer. The characteristics of spectral response functions of the filter-sensor system on GMS series satellites are a little different from one another (see Table 2), so that observed IR window radiances are different.

To eliminate this difference, the common IR window was defined as the interval between $800\ cm^{-1}$ and $950\ cm^{-1}$ and IR window radiance observed by each satellite is at first converted into this Common IR Window Radiance (CIRWR). The merit of this procedure is that after the conversion into CIRWR, the following steps to derive the total OLR are the same for each satellite.

In the case of GMS-1, 2 and 3, this regression equation is expressed as follows;

$$CIRWR = rc1_i + rc2_i * Rsat + rc3_i * Rsat^2 \quad (3.1)$$

where CIRWR: CIRWR at a given satellite zenith angle ($W/(m^2 *sr*cm^{-1})$) and

Rsat: satellite observed IR window radiance ($W/(m^2 *sr*cm^{-1})$)

i : satellite number of GMS (1, 2 or 3)

Regression coefficients rc1, rc2 and rc3 are;

	GMS-1	GMS-2	GMS-3
rc1 :	−8.2905E-4	−4.4182E-4	−9.2306E-4
rc2 :	8.4198E-1	9.4024E-1	8.3629E-1
rc3 :	9.4845E-1	3.6322E-1	9.8074E-1

The error of this estimation is as follows;

Mean Difference ($W/(m^2 *sr*cm^{-1})$)

Table 2 Normalized spectral response functions for GMS-1 and GMS-2 (W.B. Rossow et al., 1985) and GMS-3.

Wavelength (μm)	Normalized Response		
	GMS-1	GMS-2	GMS-3
9.4	0.000	0.000	0.001
9.5	0.002	0.001	–
9.6	0.002	0.002	0.001
9.7	0.002	0.002	–
9.8	0.002	0.002	0.001
9.9	0.002	0.005	–
10.0	0.002	0.008	0.007
10.1	0.004	0.046	0.045
10.2	0.020	0.262	0.225
10.3	0.104	0.691	0.534
10.4	0.355	0.881	0.637
10.5	0.675	0.937	0.686
10.6	0.871	0.982	0.764
10.7	0.943	1.000	0.822
10.8	0.947	0.962	0.881
10.9	0.944	0.966	0.946
11.0	1.000	0.954	1.000
11.1	0.941	0.835	0.988
11.2	0.904	0.664	0.959
11.3	0.857	0.529	0.967
11.4	0.789	0.430	0.957
11.5	0.704	0.341	0.953
11.6	0.652	0.289	0.957
11.7	0.578	0.241	0.949
11.8	0.508	0.193	0.913
11.9	0.489	0.155	0.849
12.0	0.471	0.116	0.813
12.1	0.466	0.097	0.793
12.2	0.465	0.088	0.796
12.3	0.451	0.080	0.763
12.4	0.414	0.067	0.787
12.5	0.404	0.058	0.749
12.6	0.429	0.043	0.456
12.7	0.372	0.014	0.196
12.8	0.210	0.009	0.073
12.9	0.088	0.001	0.027
13.0	0.033	0.000	0.012
13.1	0.000	–	–
13.2	–	–	0.004

GMS-1 : 1.1589E-17

GMS-2 : 1.1778E-17

GMS-3 : 9.8275E-18

Standard Deviation $(W/(m^2 *sr*cm^{-1}))$

GMS-1 : 5.2319E-4

GMS-2 : 1.8858E-4

GMS-3 : 5.4660E-4

3.2. Regression to Reference Satellite Zenith Angle from CIRWR

To eliminate the limb-darkening effect, CIRWR at a given satellite zenith angle is converted to the reference satellite zenith angles (sec θ = rsza = 1.00 and 1.66) through the following regression equations.

$$CIRWR_{rsza} = CIRWR_{sec\,\theta}$$
$$+ rc1 * (sec\theta - rsza)$$
$$+ rc2 * (CIRWR_{sec\,\theta} * (sec\theta - rsza)) \quad (3.2)$$
$$+ rc3 * (sec\theta - rsza)^2$$
$$+ rc4 * (CIRWR_{sec\,\theta} * (sec\theta - rsza)^2$$

where $CIRWR_{rsza}$ is CIRWR at the reference satellite zenith angle (secθ = rsza) $(W/(m^2 *sr*cm^{-1}))$ and

$CIRWR_{sec\,\theta}$ is CIRWR at a given satellite zenith angle $(W/(m^2 *sr*cm^{-1}))$. Regression coefficients rc1, rc2, rc3 and rc4 are;

	rsza = 1.00	rsza = 1.66
rc1 :	−2.2514E-3	−1.8536E-3
rc2 :	5.0459E-2	4.2475E-2
rc3 :	3.5233E-4	3.5466E-4
rc4 :	−6.4755E-3	−6.4448E-3

The error of this estimation is as follows;

	rsza = 1.00	rsza = 1.66
Mean Difference : $(W/(m^2 *sr*cm^{-1}))$	1.0315E-7	−7.3950E-8
Standard Deviation: $(W/(m^2 *sr*cm^{-1}))$	1.0588E-3	5.2454E-4

3.3. Regression to Total OLR Flux

Finally these CIRWRs at reference satellite zenith angles (secθ = rsza = 1.00 and 1.66) are converted to the total OLR flux through the following regression equations.

$$OLR = rc1$$
$$+ rc2 * CIRWR_{rsza} \quad (3.4)$$
$$+ rc3 * (CIRWR_{rsza})^2$$

where OLR is total OLR flux (W/m^2) and $CIRWR_{rsza}$ is CIRWR at the reference satellite zenith angle

Regression coefficients rc1, rc2 and rc3 are;

	rsza = 1.00	rsza = 1.66
rc1 :	9.2161E-1	9.3898E-1
rc2 :	2.2725E-3	2.1848E-3
rc3 :	−4.0212E-3	−2.9709E-3

The error of this estimation is as follows;

	rsza = 1.00	rsza = 1.66
Mean Difference : (W/m^2)	2.1595E-14	2.0885E-14
Standard Deviation: (W/m^2)	1.0198E 1	1.0017E 1

3.4 Correlations between the radiance of each longwave spectral interval and the CIRWR

To examine the effectiveness of estimating the total OLR flux from CIRWR, the correlation coefficients between the radiance of each longwave spectral interval and CIRWR were calculated and are shown in Fig. 4.

It is found that there exists rather low correlation regions corresponding to dominating absorbing bands of the atmosphere (e.g. 600—700 cm^{-1}: CO_2, 1050 cm^{-1} neighborhood: O_3/H_2O, 1500 cm^{-1} neighborhood: H_2O, 2200−2400 cm^{-1}: N_2O/CO_2). But the radiation energies from those low correlation regions are absorbed and relatively weak. As a result, the correlation coefficient between the total OLR flux obtained from radiative transfer calculations and that estimated from the regression equations using CIRWR reached 0.971 as a whole.
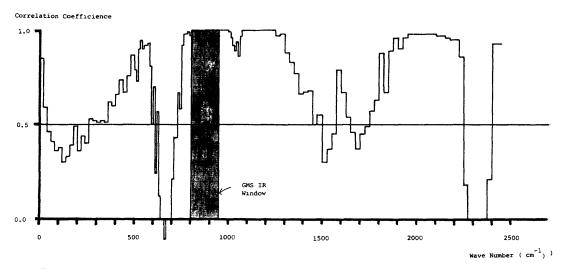
Correlation Coefficience

Fig. 4. Correlation between the radiance of each longwave spectral interval and common IR window radiance.
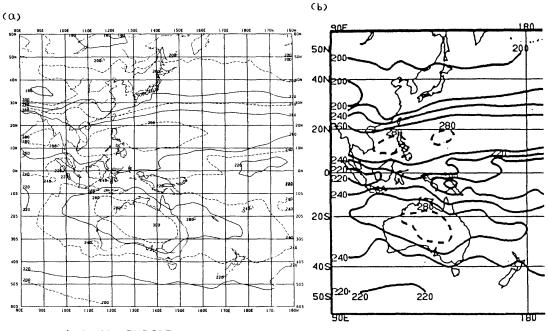
(a)

(b)

Fig. 5. (a) : GMS OLR map
(b) : NOAA OLR map (from CLIMATE DIAGNOSTIC BULLETIN) for March 1987

4. Some Examples of the Estimation

Monthly mean GMS OLR flux data set, averaged over 2.5 degrees latitude by 2.5 degrees longitude boxes, has been derived experimentally since March, 1987 and sub-sequently processed into map. These maps have been compared with NOAA OLR map as a reference, which is derived from NOAA 9 AVHRR IR window radiance measurements by NESDIS/ESL, for the verification of our esti-
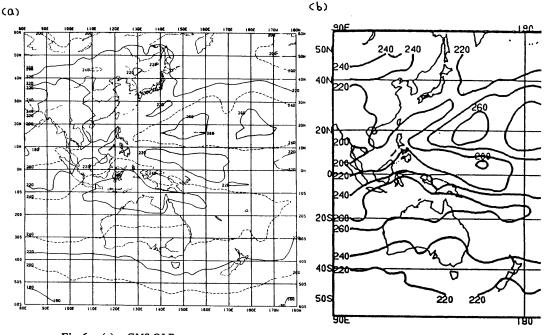
(a)

(b)

Fig. 6. (a) : GMS OLR map
(b) : NOAA OLR map (from CLIMATE DIAGNOSTIC BULLETIN) for June 1987

mation algorism. Fig. 5 shows the example for March 1987; (a) GMS OLR map and (b) NOAA OLR map, and Fig. 6 shows the example for June 1987. It is found that the pattern is quite similar, but the maxima are overestimated in March and underestimated in June.

5. Conclusion

This paper described a method for estimating Outgoing Longwave Radiation flux from GMS Infrared window radiances. The estimating algorism has been tested and adjusted since March 1987, and it has been shown that GMS OLR can be used as a substitute for NOAA OLR. By using GMS OLR data set, the OLR flux distribution pattern can be monitored on real time basis.

Another merit of GMS OLR data set is that the data set are made for 3-hourly observations; namely 00, 03, 06, 09, 12, 15, 18 and 21 UTC, so that diurnal variation of OLR pattern is

well captured through GMS OLR.

6. Acknowledgements

The authors wish to thank Dr. Phillip A. Arkin for his encouragement of this work and Mr. John Janowiak for his kind offering of the NOAA OLR data on CCT.

References

McClatchey, J.N., Benedict, W.S., Clough, S.A., Burch, D.E., Calfee, R.F., Fox, K., Rothman, I.S. and Garing, J.S. (1973): Atmospheric absorption line-parameters compilation. AFCRL-TR-73-0096, Environ. Res. Pap., 434, 78 p.

Rodgers, C.D. and Walshaw, C.D. (1966): The computation of infra-red cooling rate in planetary atmospheres. Q.J.R. Meteorol. Soc., 92, 67-92.

William, B., Rossow, Edward, Kinsella, Audrey, Wolf and Leonid, Garder (1985): International Satellite Cloud Climatology Project (ISCCP) Description of Reduced Resolution Radiance Data (Draft). WMO/ICSU.

YAMANOUCHI, T., YAMAMOTO, Y., MESHIDA, S. and UCHIYAMA, A. (1981): On the Measurements by Radiometersonde at SYOWA Station, Antarctica. Memoirs of National Institute of Polar Research Special Issue No. 19. Proceedings of the This Symposium on Polar Meteorology and Glaciology.

GMS で観測された赤外窓領域の放射強度から
外向き長波長放射フラックス（OLR）を推定する試み

操野年之*，内山明博**

　GMS で観測された赤外窓領域の放射強度から，OLR を回帰式により指定した。

　この回帰式の係数は，種々の大気の状態のもとでの放射伝達モデルの計算結果から求めた。

　この調査では，140の大気状態について，それぞれ 8 方向の衛星天頂角に対する放射強度を求めた。このモデル計算の結果，GMS の窓領域に相当する放射強度と OLR の間には，高い相関（R=0.971）があることがわかったが，水蒸気や二酸化炭素等の吸収帯に相当する部分との相関は低かった。